



Proceedings of the Seventeenth International Conference on  
Civil, Structural and Environmental Engineering Computing  
Edited by: P. Iványi, J. Kruis and B.H.V. Topping  
Civil-Comp Conferences, Volume 6, Paper 13.5  
Civil-Comp Press, Edinburgh, United Kingdom, 2023  
doi: 10.4203/ccc.6.13.5  
©Civil-Comp Ltd, Edinburgh, UK, 2023

# Complexity Adaptation Strategy for Order-Adaptive Elements

E.D. Mora<sup>1,2</sup> and N. Khaji<sup>1</sup>

<sup>1</sup>Graduate School of Advanced Science and Engineering,  
Hiroshima University, Japan

<sup>2</sup>Departamento de Ingeniería Civil y Ambiental, Escuela  
Politécnica Nacional, Ecuador

## Abstract

Many studies have worked on reducing dynamic analysis convergence problems. Currently, there are some robust algorithms. However, they can fail when dealing with complex structures due to numerical and especially physical instabilities. Some of them can also be time-consuming procedures. On the other hand, the intrinsic truncated error in structural analysis decreases when the shape function order is raised (p-refinement). Nevertheless, this action will increase the complexity and, thus, structural convergence problems. Therefore, the solution proposed is to adapt the complexity when physical instabilities are predicted, and Hermite interpolation can be used to state well-posed results. The physical instability can be predicted by analyzing strain energy outliers and moment-curvature rule abnormalities. Moreover, to get more realistic results, nonlinear elements with plastic length were developed. Since no previous references have worked with these kinds of nonlinear high-order elements, using a set of sigmoid functions in the stiffness matrix integral was the solution to obtain generalized high-order Timoshenko beams. Another contribution of this work was establishing an appropriate manner of getting the maximum permissible error in p-adaptive methods. Finally, some examples were made to prove the formulation's robustness and show how influential the truncated error can be.

**Keywords:** frame elements, high-order elements, nonlinear elements, p-adaptive

## 1 Introduction

Although forces equilibrium and displacement compatibility are guaranteed among

all degrees of freedom (DOF) in structural analysis, for reliable results, the consistency between the equilibrium-compatibility analysis and the interpolation functions must also be satisfied. Lack of this consistency can lead to significant truncation errors. Thus, a solution is to increase the number of elements ( $h$ ) or the order of the interpolation functions ( $p$ ). A new problem arises from there; the complexity system, round-off error, and analysis time increase too. Complexity is a characteristic of actual buildings that can lead to significant challenges, for it will result in a lower analysis convergence rate if it is combined with high nonlinearities. The objective of this work is to establish a robust and no time-consuming procedure that can deal with dynamic analysis reducing the truncated error.

The truncated error can be reduced using h-, p-, or hp-adaptive methods, where only the more influential elements will be refined. The p-adaptive methods can reduce the truncated system error more efficiently than the h-adaptive methods since the number of DOFs will be minor. For instance, for the analyzed buildings in the present study, some elements should be divided into ten times more parts by using an h-adaptive method instead of a p-adaptive. This fact is also important because the higher the DOF number, the higher the system complexity. Hence, this study will focus on p-adaptive approaches.

One of the biggest concerns is to get numerical and physical stability on complex systems. There are many researchers that have worked to reduce this convergence problem for dynamic analysis. For example, we have in the last years the followings. Abuteir, Harkati, Boutagouga, Mamouri, and Djefhaba [1] worked with soft higher-order deformation modes using a reduced/selective numerical on functionally graded material plates. For this purpose, they employed a five-point reduced integration scheme in membrane and shell elements to prevent the zero energy hourglass mode phenomenon. Moreover, an implicit time integration based on a combination of the trapezoidal rule and the three Euler backward methods was used to achieve convergence when nonlinearities occur. Some other authors have developed time integration schemes, like Song, Eisenträger, and Zhang [2] or Ji and Xing [3], who based their studies on a space-state formulation. Aside from time high-order methods, the Generalized-alpha approaches, which are faster than others, can reduce spurious frequencies that can produce a system divergence. However, Generalized-alpha methods cannot guarantee the conservation of energy-momentum, which can evocate in a system instability too [4]. Otherwise, the state space-based procedures might consume time since the second-order differential equation needs to be converted into a first-order differential equation, which generally results in a matrix twice the size of the total stiffness matrix. Therefore, the present study will use Generalized-alpha methods, and the energy-momentum conservation will be controlled indirectly.

The next issue is to obtain a realistic nonlinear model, e.g., frames with plastic lengths, for high-order shape function elements. No current studies present a solution for this specific problem. However, the closest related studies are stated in the following. Park and Kim [5] and Kim, Son, Yi, and Hong [6] created a procedure for nonlinear analysis in plastic regions. They worked with a force-based element and Lagrangian shape functions. In their proposal, the authors use polynomial enrichment

functions in the plastic region to represent nonlinear occurrence. It has been shown herein that discontinuities can be added to the material nonlinearity, avoiding enrichment functions.

Eisenträger, Atroshchenko, and Makvandi [7] observed the influence of increasing the polynomial order of the element compatibility function and, for the same reason, of the shape function. They worked with only elastic systems and static forces with 1D (rod element), 2D, and 3D elements. Bai, Gao, Liu, and Chan [8] have proposed a nonlinear beam-column element with 16 degrees of freedom. In another study, since there are only a few papers dealing with the task of improving the performance of elements, Sharifnia [9] worked on a theory for a high-order element for large deformations. Hence, the solution for obtaining nonlinear plastic length on high-order elements was to use a set of sigmoid functions to depict the nonlinear material behavior conserving the continuous displacement space on generalized Timoshenko elements.

The contributions presented herein are to have set out 1) a robust time-history procedure based on an adaptive complexity scheme that can reduce the truncated error, 2) a stiffness matrix process that can deal with nonlinear plastic length hinges on high-order elements, and 3) an effective manner to obtain the maximum permissible error for p-adaptive (and h-adaptive) procedures.

## 2 Methods

The convergence of the solution for every iteration of a nonlinear differential equation set analysis will be affected by the stiffness, mass, and damping matrices, the applied loads, and the analysis method used. The matrices and applied loads can be affected by the system's complexity. The general approach of this study will be to adapt the system complexity to reduce the convergence problems when high nonlinearities occur. The complexity of structural analysis ( $C$ ) can be summarized by the set of nodes ( $N$ ), set of elements ( $E$ ), set of degrees of freedom ( $DOF$ ), material properties ( $M$ ) (because composites or viscoelastic materials will need more complex analysis), the set of loads ( $L$ ), and set of boundary conditions ( $BC$ ). If we let  $C$  be a tuple such as  $C = (N, E, DOF, M, L, BC)$ , and  $\bar{C}$  is a complexity enough to achieve convergence, the condition  $C \leq \bar{C}$  shall be met for a successful analysis.  $C$  will increase when p- or h-refinement is employed because  $N$ ,  $E$ , and  $DOF$  will do too. Therefore, a scheme that reduces  $C$  using Hermite interpolation to ensure well-posed results has been proposed. In addition, other techniques have been studied and described below.

### 2.1 Structural Analysis Procedure

The lack of convergence from high-order shape functions can arise for large time-step sizes, which causes numerical instability. Consequently, implicit time-history analysis is more convenient for the problem of this study. As stated before, some of the faster and more robust procedures are the Generalized-alpha methods (GAM). Those belong to the direct integration implicit procedures that were derived from the Newmark type

analysis. Therefore, GAM will be used with a modification to reduce physical instability for high-order interpolation functions.

The physical instability problem will be predicted when 1) the strain energy  $\hat{\mathbf{u}}^e_i$  (see Equation (1)) in the time-step  $i$  is an outlier. Also, when 2) an abnormal behavior is identified in the moment-curvature rules, e.g., the Roufaiel and Meyer concrete model. It is important to consider smoothing all the element rigidity changes in the same direction.

$$\hat{\mathbf{u}}^e_i = \frac{1}{2} \mathbf{d}^e_i{}^T K^e_i \mathbf{d}^e_i \quad (1)$$

Let  $\mathbf{d}^e$  be the displacements in the element  $e$  DOFs and  $K^e$  be the element stiffness matrix.

The method used to find outliers corresponds to the one developed by Grubbs, as this method has been greatly validated [10]. The expression (2) summarizes the Grubbs procedure. Thus, if some value does not meet the inequality, it will be considered an outlier.

$$T_n(b, \beta) = \frac{b_n - \bar{b}}{\sqrt{\frac{\sum_{i=1}^n b_i^2 - (\sum_{i=1}^n b_i)^2}{n(n-1)}}} \leq \frac{t_{\beta/n, n-2}}{\sqrt{1 + \frac{nt_{\beta/n, n-2}^2 - 1}{(n-1)^2}}} \quad (2)$$

In Equation (2),  $n$  is the size of a general list  $b$ ,  $\beta$  is the significance, e.g.,  $\beta = 0.1$ ,  $t_{\beta/n, n-2}$  is the statistical  $t$  of Student with a significance scaled by the number of samples and a degree of freedom (different from the structural DOFs) equal to  $n - 2$ .

## 2.2 Nonlinear Plastic Length for High-Order Element

An important contribution of this work has been to develop a fashion to calculate the stiffness matrix of an element with different constant rigidities along it. The solution was to transform the problem basis. The flexibility method in nonlinear analysis obtains an equivalent unique stiffness element using in-series approaches. That is why the stiffness's integral limits of  $K^e = \int_0^L \mathbf{B}^T \mathbf{D} \mathbf{B} \partial x$  cannot change when different rigidities exist; if they do, incoherent results will be obtained. Rather the unique stiffness element has to be converted into an in-parallel problem by using continuous functions to represent the rigidity variations appropriately. For that reason, the more suitable functions used were a set of Sigmoid curve functions. Therefore, Equation (3) can be applied.

$$K^e = \sum_{r=1}^{\bar{n}-1} \int_0^L \mathbf{B}^T \mathbf{D}_r \mathbf{B} \partial x \quad (3)$$

$$\mathbf{D}_r = \begin{bmatrix} \overline{EI}_{y_1} + \Delta \overline{EI}_{y_r} \sigma(x - \sum_{g=1}^r l_g) & 0 \\ 0 & \left( \frac{EI_y}{\phi_c L^2} \right)_r \end{bmatrix} \quad (4)$$

Let  $r$  and  $g$  be the segment numbering,  $\overline{EI}_y$  be the segment element rigidity in local axis  $y$ ,  $\Delta\overline{EI}_{y_r}$  equals  $(\overline{EI}_{y_{r+1}} - \overline{EI}_{y_r})$ ,  $\bar{n}$  be the number of element segments,  $l$  be the segment length,  $\sigma(\cdot)$  be the sigmoid function expressed as  $\sigma(a) = \frac{1}{1+e^{-|\overline{EI}_{\max}|(a)}}$ , and  $\phi_c L^2$  be the section shear coefficient multiplied by the element length.

Equation (3) states the general expression of a Timoshenko element which can be solved by the Gauss quadrature integration method; here, the nodes and Gauss points do not need to coincide. In the interest of simplifying the diverse equations and consequent algorithms, the Barlow points are not being used. Yet, the usage of the number of DOFs in every plane has proved to be enough to obtain accurate results.

By substituting Equation (3) into (1), we can obtain the energy in the plastic length region (see Equation (5)).  $m_r^e$  from Equation (5) turns out to be the moment evaluated in the moment-curvature diagram.

$$\hat{\mathbf{u}}_{i_r}^e = \frac{1}{2} \mathbf{d}_i^e T \left( \int_0^L \mathbf{B}^T \mathbf{D}_r \mathbf{B} dx \right)_i \mathbf{d}_i^e = \frac{1}{2} \mathbf{d}_i^e T m_{r_i}^e \quad (5)$$

### 2.3 Additional Techniques

Other three well-known procedures can be used to increase the analysis stability. Because high-order interpolation functions can result in spurious frequencies, Ritz modal shapes using the straightforward Gram-Schmidt process can prevent the excitation in directions that do not need to be studied. Aside from that, regarding the Runge phenomenon, a different distribution of nodes from equidistant locations should be used, like Lobatto, Legendre, or Chebyshev approaches. Previous works have shown remarkable results with the Lobatto and Chebyshev node distributions for high-order interpolations. Finally, a Reduced Integration scheme can be used in some elements to improve the stability and accuracy of the solution. In a typical finite element analysis, the governing equations are integrated over each element in the mesh using a numerical integration scheme, such as Gauss quadrature. The integration order is typically chosen to be equal to the polynomial order of the shape functions to ensure that the integral is exact for polynomials of that order. However, this can lead to numerical instability for problems with high-order shape functions, particularly if the mesh is not sufficiently refined. The reduced integration method involves using a lower-order numerical integration scheme to solve the governing equations, typically one or two orders lower than the full integration order.

### 2.4 P-Adaptive Method for Frame Structures

The shape functions for structural analyses were developed by interpolating the internal DOF displacements, and it is assumed that the same functions are used to interpolate the internal DOF forces, see Equation (6).

$$\bar{\mathbf{m}}_y^* = \underline{\mathbf{N}} \mathbf{m}_y^* \quad (6)$$

Let  $\bar{\mathbf{m}}_y^*$  be the continuous equation of the element moments in the local axis  $y$ ,  $\underline{\mathbf{N}}$  be the shape functions, and  $\mathbf{m}_y^*$  be the prescribed moments in the element DOFs.

The assumption taken in (6) is made since it is considered every element segment embraces a linear correspondence between displacement and forces, even in nonlinear analyses, for every iteration uses a corresponding linear force-displacement relation. Internal forces of the element can also be calculated with constitution and kinematics considerations, as stated in Equation (7).

$$\bar{\mathbf{m}}_y \approx \mathbf{D}\mathcal{L}_2\underline{\mathbf{N}}\mathbf{d}^{xz} \quad (7)$$

The truncated error can be calculated using (8), and the base of p-adaptive methods is to reduce that error subsequently normalized.

$$e_m \approx \bar{\mathbf{m}}_y^* - \bar{\mathbf{m}}_y \quad (8)$$

In linear analyses, the maximum permissible error  $\bar{\eta}$  will be established after various iterations (see Equation (9)). Nonetheless, in nonlinear analyses or time-history analyses,  $\bar{\eta}$  can be obtained within the first steps of the procedures, where the global results will not be affected.

$$\bar{\eta} \approx \max_{i \in n} T_n \left( \sum_{el=1}^{nel} \frac{e_{m_{el}}}{m_{y_{el}}}, \beta \right)_{n \times 1} \quad (i) \quad (9)$$

The maximum permissible error determination has been a problem solved differently by other authors [11]. In this work, the problem identified was that the internal forces of some elements could tend to zero, so the related results of  $\bar{\eta}_0$  will tend to be infinitive, which will bring spurious outcomes. For that reason, the effectively proven proposal is that outliers' values have to be discarded from  $\bar{\eta}_0$ . The method used corresponds to the one developed by Grubbs, stated in Equation (2).

Once  $\bar{\eta}$  is get, the permissible error  $\bar{e}_{nel}$  is obtained using the total displacement divided by the number of elements  $nel$  as indicated in Equation (10), where  $nel$  is the number of elements. Finally, the error can be calculated using the discrete Sobolev space norm and later normalized in  $\xi^e$ , in such a way that an optimal order  $p$  or number of element divisions  $h$  can be found if  $\xi^e = 1$ .  $\xi_{el}$  is calculated with (10).

$$\xi^e = \frac{\left( \sum_{el=1}^{nel} e_m^T e_m \right)^{\frac{1}{2}}}{\bar{\eta} \left[ \frac{\|d^{xz}\|^2 + \sum_{el=1}^{nel} e_m^T e_m}{nel} \right]^{\frac{1}{2}} \leq \|e\|_{el}} \quad (10)$$

If  $\xi^e > 1$  the order must be refined.

## 2.5 Pseudo-Algorithm

As described before, the proposal of this study is to use an adaptive system complexity based on Hermite interpolation to reduce and restore the additional internal nodes in the elements to reduce the complexity system  $\mathcal{C}$ . Table 1 states the pseudo-algorithm for time-history analysis with high-order interpolation functions. The new variables presented are the system responses  $q_i, \dot{q}_i, \ddot{q}_i$ ; they correspond to the system

displacement, velocity, and acceleration.  $GIOR^e$  is the element's Gauss Integration Order Reduction number. Furthermore, the Round-off error normalized to one can be calculated using Equation (11) where  $\bar{\kappa}(M^{-1}K)$  is the condition number of the system inverted mass and stiffness matrices, and  $\varepsilon$  is the Machine Epsilon number.

$$\varepsilon_{Round-off} = \bar{\kappa}(M^{-1}K)\sqrt{\varepsilon} \quad (11)$$

**Procedure Algorithm for Structural Time-history Analysis**

```

1: begin
2:   Initialize variables
3:    $C_{num} = 0$ 
4:    $refine = True$ 
5:    $GIOR^e = 0$ 
6:   for all ground motion points  $i$ :
7:     Ritz modes decomposition
8:     using the Generalized Alpha method with Newton-Raphson:
9:      $q_i, \dot{q}_i, \ddot{q}_i \leftarrow$  for principal DOFs and internal nodes using  $q_{i-1}, \dot{q}_{i-1}, \ddot{q}_{i-1}$ 
10:     $K^e_i \leftarrow$  evaluated with Moment-Curvature curves, considering  $GIOR^e$ , and Equation (3)
11:     $m_{r_i}^e \leftarrow$  from Moment-Curvature evaluation
12:    if the Moment-Curvature evaluation has an unexpected behavior:
13:       $\varepsilon_r^e = True$ 
14:    else:
15:       $\varepsilon_r^e = False$ 
16:       $\hat{u}^e_i \leftarrow$  using Equation (6)
17:      if  $\xi_{el} > 1 + tolerance_1$  and  $refine == True$ :
18:         $internal\ nodes^e = f(\xi^e)$ 
19:         $q_i, \dot{q}_i, \ddot{q}_i \leftarrow$  for principal DOFs and for internal nodes using interpolation
20:      else:
21:         $refine = False$ 
22:        if  $\varepsilon_{Round-off} > 1 + tolerance_2$ :
23:          Break all
24:         $C_{num} = C_{num} - 1$ 
25:        if ( $\hat{u}^e_i \geq tolerance_3$  or  $\varepsilon_r^e == True$ ) and  $C_{num} \leq 0$ :
26:           $GIOR^e = 1$  or  $2$ 
27:          if  $\varepsilon_r^e == True$ :
28:             $C_{num} = 4$ 
29:             $q_i, \dot{q}_i, \ddot{q}_i \leftarrow$  only keeping the responses of the principal DOFs
30:          else if  $C_{num} == 1$ :
31:             $q_i, \dot{q}_i, \ddot{q}_i \leftarrow$  for principal DOFs and for internal nodes using interpolation

```

Table 1: Procedure Algorithm for structural time-history analysis.

### 3 Results

For this paper, the tested buildings are made of concrete, where the moment-curvature curves were found using the procedure described in Monti and Petrone [12]. Additionally, the pinching effect was considered to prove the proposed formulation's robustness. Furthermore, the structural responses were compared with OpenSees or Seismostruct for validation. About the external loads, the ground motions used were filtered and line-base corrected. The earthquakes used were Concepción-Chile (2010) and Tohoku-Japan (2011) ground motions because they produced naturally strong shakes and had different main frequencies. The selected earthquakes meet two desired

conditions: 1) large accelerations that take the structure into a nonlinear range and 2) different frequencies that help to verify the formulation robustness. The main frequencies obtained from a Fast Fourier procedure of the Concepción ground motion are between 0.30 Hz and 1.95 Hz, and the Tohoku motion is 4.30 Hz.

The examples presented in this paper are made of concrete with a 21881978.89 KN/m<sup>2</sup> Young modulus, 21000 KN/m<sup>2</sup> stress, 24 KN/m<sup>3</sup> specific weight, and 590000 KN/m<sup>2</sup> yield stress rebars. The buildings use an additional reactive weight of 7.5 KN/m<sup>2</sup>, and their elements were sized in such a way that the structural system passes into the nonlinear range, as follows:

Building 1): One-floor 3D regular building with one span.

Building 2): Four-floor 3D regular building with two spans.

Building 3): Six-floor 3D irregular building with metallic energy dissipation devices.

The following results are the most significant for the problem posed.

1) Figure 1 presents the number of function orders vs. the truncated error average of the elastic structural behavior instants of the time history analyses for Building 1, 2, and 3. It is interesting to appreciate that all the curves have the same tendency. Without internal nodes (second order), the error is a very large number that could be a problem for h-adaptive methods. Then, we can see that the error increases with one internal node (four order), and in all the cases, the error decreases to values near one and zero after two internal nodes (sixth order).

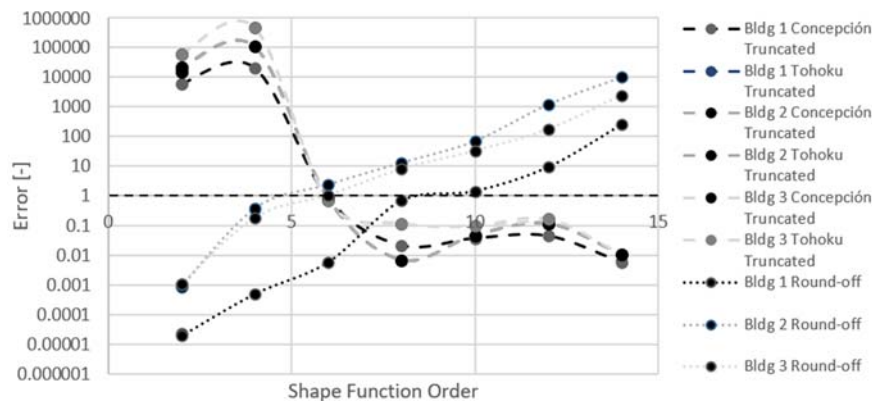


Figure 1: Truncated and round-off error of Buildings with real ground motions.

2) Because Building 3 shows greater variability in its response to the Concepción earthquake, only its results are presented in Figure 2. Figure 2a shows the displacement of the building's roof vs. the time.

3) Figure 2b shows a schematic representation of structural damage on the irregular building for the second order and an order using p-adaptive methods. The black segments in Figure 3 indicate that the element end has yielded. The Concepción ground motion was used for this example because its frequencies produced more damage to the structures proposed. With p-adaptive methods, principal columns and beams needed two additional nodes, and the rest of the elements remained without



internal nodes. There is different damage in one column, sixteen beams, and two braces.

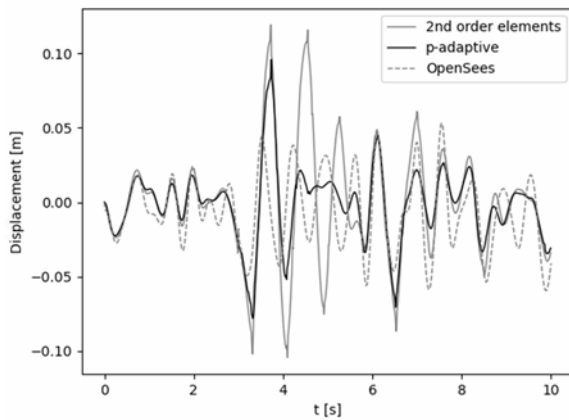


Figure 2a

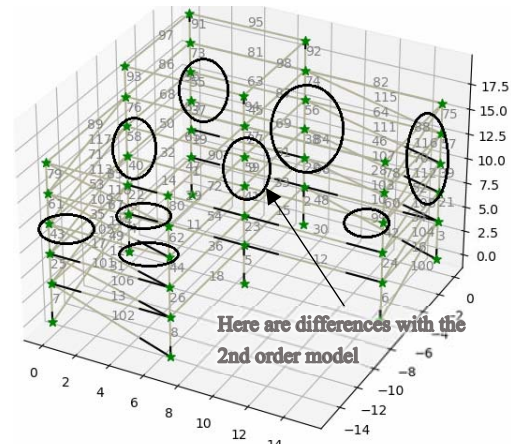


Figure 2b. p-adaptive

Figure 2: Irregular building results (Building 3). Figure 2a. Roof displacement vs. time. Figure 2b. Structural damage differences between p-adaptive and 2<sup>nd</sup>-order elements.

## 4 Conclusions and Contributions

This work exposed an error based on truncation for the shape function order. This error is not usually checked in structural analyses, which are the typical calculations for buildings, bridges, and other infrastructures. That is why a general procedure for a Timoshenko high-order element was presented. As well the equations used to determine the truncated error were presented. Because there are no studies that show how to calculate a nonlinear plastic length on a high-order element, a simple way was introduced using sigmoid function sets. Additionally, an adaptive procedure was studied.

For the p-adaptive method, the process of normalizing the truncated error, the maximum permissible error can tend to the infinitive, so a procedure to identify outlier values was proposed and verified with the examples posed.

In the examples, it was found that in all the cases, the optimum number of additional internal nodes is two or three, and if less than two nodes are considered, the produced error is a large value. Additionally, it was shown that there could be differences from the structural responses when the truncated error is reduced.

Generally, dynamic analyses applied to complex structures with high nonlinearities can produce physical instability. The property of complexity was defined in this work, and herein was shown that this property increases when the elements are refined. Therefore, this study has posed a process to adapt the complexity according to possible physical instabilities identified by controlling the element potential energy and moment-curvature abnormalities. The change of complexity was made through Hermite interpolations.

## References

- [1] B. W. Abuteir, E. Harkati, D. Boutagouga, S. Mamouri, and K. Djeghaba, “Thermo-mechanical nonlinear transient dynamic and Dynamic-Buckling analysis of functionally graded material shell structures using an implicit conservative/decaying time integration scheme,” *Mechanics of Advanced Materials and Structures*, vol. 29, no. 27, pp. 5773–5792, 2022.
- [2] C. Song, S. Eisenträger, and X. Zhang, “High-order implicit time integration scheme based on Padé expansions,” *Comput Methods Appl Mech Eng*, vol. 390, no. 2022, pp. 1–43, Feb. 2022, doi: 10.1016/j.cma.2021.114436.
- [3] Y. Ji and Y. Xing, “A two-step time integration method with desirable stability for nonlinear structural dynamics,” *European Journal of Mechanics, A/Solids*, vol. 94, no. 2022, pp. 1–19, Jul. 2022, doi: 10.1016/j.euromechsol.2022.104582.
- [4] M. Lavrenčič and B. Brank, “Comparison of numerically dissipative schemes for structural dynamics: Generalized-alpha versus energy-decaying methods,” *Thin-Walled Structures*, vol. 157, no. 2020, pp. 1–22, Dec. 2020, doi: 10.1016/j.tws.2020.107075.
- [5] K. Park, H. Kim, and D. J. Kim, “Generalized Finite Element Formulation of Fiber Beam Elements for Distributed Plasticity in Multiple Regions,” *Computer-Aided Civil and Infrastructure Engineering*, vol. 34, no. 2, pp. 146–163, Feb. 2019, doi: 10.1111/mice.12389.
- [6] D. J. Kim, H. J. Son, Y. Yi, and S. G. Hong, “Generalized finite element formulation for efficient first-order plastic hinge analysis,” *Advances in Mechanical Engineering*, vol. 11, no. 3, Mar. 2019, doi: 10.1177/1687814019836366.
- [7] S. Eisenträger, E. Atroshchenko, and R. Makvandi, “On the condition number of high order finite element methods: Influence of p-refinement and mesh distortion,” *Computers and Mathematics with Applications*, vol. 80, no. 11, pp. 2289–2339, Dec. 2020, doi: 10.1016/j.camwa.2020.05.012.
- [8] R. Bai, W. L. Gao, S. W. Liu, and S. L. Chan, “Innovative high-order beam-column element for geometrically nonlinear analysis with one-element-per-member modelling method,” *Structures*, vol. 24, pp. 542–552, Apr. 2020.
- [9] M. Sharifnia, “A higher-order nonlinear beam element for planar structures by using a new finite element approach,” *Acta Mech*, vol. 233, no. 2, pp. 495–511, Feb. 2022, doi: 10.1007/s00707-021-03076-4.
- [10] ASTM E178, “Dealing With Outlying Observations 1,” 2016. doi: 10.1520/E0178-08.Copyright.
- [11] H. Moslemi and A. Tavakkoli, “A Statistical Approach for Error Estimation in Adaptive Finite Element Method,” *International Journal for Computational Methods in Engineering Science and Mechanics*, vol. 19, no. 6, pp. 440–450, Nov. 2018, doi: 10.1080/15502287.2018.1558424.
- [12] G. Monti and F. Petrone, “Yield and Ultimate Moment and Curvature Closed-Form Equations for Reinforced Concrete Sections,” *ACI Struct J*, vol. 112, no. 4, 2015, doi: 10.14359/51687747.